Ultrahigh Refractive Index Sensitivity With Lossy Mode Resonance in a Side-Polished Low-Index Polymer Optical Fiber

Juan David Lopez, Ignacio R. Matias, *Fellow, IEEE*, Marcelo Martins Werneck, Regina Célia da Silva Allil, and Ignacio Del Villar

***Abstract*— This work presents a theoretical–experimental study of a refractive index (RI) sensor based on lossy mode resonances (LMRs) generated with a side-polished low-index polymer optical fiber. The theoretical part involves conducting simulations to determine the optimal coating thickness for achieving the first (1st) and second (2nd) LMR, as well as to determine their respective sensitivities. In the experimental part, a cyclic transparent fluoropolymer optical fiber is used, which is first polished and then coated with tin oxide (SnO_2) thin film to obtain the LMR. The simulated and experimental results exhibit a high level of agreement. In the visible light spectrum region, the sensitivities for the first LMR are, respectively, 11 300 nm/RI unit (RIU) and 15 973 nm/RIU within the RI range of 1.333–1.345. Similarly, for the second LMR, the sensitivities are, respectively, 520 and 467 nm/RIU within the same RI range. Furthermore, experiments conducted in the near-infrared light spectrum region show a record sensitivity of 57 200 nm/RIU, while the second LMR exhibits a sensitivity of over 5 000 nm/RIU within the RI range of 1.340–1.345. These results underscore the potential of utilizing cyclic transparent optical polymer (CYTOP) fiber in various applications requiring the detection in liquid samples, such as biosensors or chemical sensors.**

***Index Terms*— Lossy mode resonance (LMR), low-index polymer optical fiber, refractive index (RI) sensor, side-polished optical fiber.**

I. Introduction

THE measurement of fluid refractive index (RI) is a topic of great interest in modern sensing technologies, as it allows the quantification and monitoring of various key variables, such as pressure, temperature, bacteria, additives, contaminants, antigens, and antibodies [1], [2]. Consequently, RI-based sensors play a vital role across a wide array of applications in biology [3], diagnostics [4], petroleum engineering, environmental monitoring, and food quality assessments [5], [6].

Numerous optical technologies have been proposed to effectively monitor the RI of liquids. Among these, optical fiber sensors have garnered significant attention owing to their advantages over other technologies [2], [7], [8]. Optical fibers offer several remarkable benefits, including intrinsic electrical isolation, immunity to electromagnetic interference, and the ability to monitor sensors remotely and the potential for miniaturization, which is important in the field of diagnosis, where very small liquid quantities must be used [9], [10].

Among RI sensors based on optical fiber, we can mention several structures that have been studied in the last decade: single-mode–multimode–single-mode (SMS) fibers [11], Fabry-Perot and etched fiber Bragg grating (eFBG) [12], tilted fiber Bragg gratings (TFBGs) [13], D-shaped polished fibers [10], multimode fiber all core [14], and plastic optical fibers (POFs) [15]. In certain structures, it is possible to measure the RI using both light power (intensity) and wavelength shift. One such example is the all-core multimode fiber, which can be polished to perform the measurement based on the changes in light power or coated with a film to enable sensing through resonance wavelength shifts. In the case of the latter, metals, such as gold or silver, are commonly employed to induce surface plasmon resonance (SPR) [16]. Meanwhile, metallic oxides are typically used to generate lossy mode resonance (LMR) [17]. Unlike SPR, LMR is not restricted by thickness, and its resonance can be easily tuned. Furthermore, the use of almost any metal oxide to generate the LMR increases the range of applications in which it can be studied.

In recent years, there has been growing focus on studying LMR resonances with the aim of enhancing their sensitivity and establishing them as a cost-effective alternative to conventional biosensors [4]. The sensitivity of the LMR depends on several factors, primarily the film thickness, the central wavelength of LMR, and the RI of the fiber core. Researchers have reported that increasing the thickness of the film on optical fiber results in a shift of the peak LMR toward the

Manuscript received 5 September 2023; revised 1 November 2023; accepted 12 November 2023. Date of publication 1 December 2023; date of current version 29 December 2023. This work was supported in part by the Coordenação de Aperfeiçoamento de Pessoal de Nível Superior—Brasil (CAPES)—Finance Code 001 ("doutorado sanduiche"); in part by the Human Resources Program (PRH) of the Brazilian National Agency of Petroleum, Natural Gas and Biofuels under Grant PRH-16.1; and in part by the Government of Navarre through its Project under Grant 0011-1365-2022-000241. The Associate Editor coordinating the review process was Dr. Guanfeng Du. *(Corresponding author: Ignacio Del Villar.)*

Juan David Lopez is with the Nanotechnology Engineering Research Program, Federal University of Rio de Janeiro, Rio de Janeiro 21941598, Brazil (e-mail: juandlopezv94@gmail.com).

Ignacio R. Matias and Ignacio Del Villar are with the Electrical, Electronic and Communications Engineering Department and the Institute of Smart Cities (ISC), Public University of Navarre, 31006 Pamplona, Spain (e-mail: natxo@unavarra.es; ignacio.delvillar@unavarra.es).

Marcelo Martins Werneck and Regina Célia da Silva Allil are with the Electrical Engineering Research Program, Federal University of Rio de Janeiro, Rio de Janeiro 21941598, Brazil (e-mail: werneck@coppe.ufrj.br; reginaceliaallil@gmail.com).

This article has supplementary downloadable material available at https://doi.org/10.1109/TIM.2023.3338653, provided by the authors.

Digital Object Identifier 10.1109/TIM.2023.3338653

infrared range, which leads to an enhanced sensitivity of the sensor.

Among the most studied metallic oxides to generate the LMR effect on optical fiber, we can mention AZO, IGZO, ZnO, In_2O, TiO_2, SnO_2, ITO, CuO, and ZrO_2 [18], [19]. Experimentally, these materials deposited on a multimode optical fiber have generated sensitivity ranging from 880 nm/RI unit (RIU) to 13 000 nm/RIU. In this context, Sanchez et al. [20] conducted a study with the objective of determining the sensitivity of each order of the LMR, ranging from the first (1st) order to the seventh (7th) order. To achieve this, they utilized a 200-μm multimode fiber coated with a SnO_2 film. The results of the study demonstrated the stability of SnO_2 over time, revealing sensitivities ranging from 185 to 5390 nm/RIU. Notably, the lowest sensitivity was observed for the 7th-order LMR, while the highest sensitivity was recorded for the 1st order.

With the aim of enhancing the sensitivity of LMR-based sensors, the utilization of materials with low RI has been proposed [21]. Among these materials, fluorinated polymers have emerged as remarkable due to their properties that make them well-suited for sensor applications. These properties include high transparency, thermal stability, and infrared transmission. Among the fluorinated polymers studied in the literature, two notable examples are tetrafluoroethylene perfluoro (PFA) and cyclic transparent optical polymer (CYTOP) [11], [22], [23]. In this regard, in 2023, Dominguez et al. [24] reported the fabrication of a refractometer utilizing a PFA substrate coated with an ITO thin film in a planar waveguide configuration. The results of this study confirm that by employing PFA (a low RI material) deposited with the 1st-order LMR of ITO, a sensitivity of up to 41 000 nm/RIU was achieved. In contrast, the 2nd-order LMR exhibited an average sensitivity of 1750 nm/RIU. Both LMRs were studied within the near infrared (NIR) region.

In a similar vein to utilizing materials with a low RI, Cao et al. [23] conducted a study on a refractometer by employing SPR instead of LMRs. They used a side-polished CYTOP optical fiber coated with a 55-nm gold thin film. Experimental results indicated that when characterizing the sensor in the NIR region, the proposed sensor achieved a sensitivity of approximately 23 000 nm/RIU.

The results reported in the literature, utilizing PFA (flat substrate) and CYTOP fiber, validate the rule that suggests that as the RI of the substrate and the RI of the surrounding medium approach each other, the sensitivity increases [21]. This idea was further confirmed with analytical equations, which theoretically indicate that the sensitivity becomes infinitely high when both RIs are equal [17].

Given the remarkable sensitivities achieved using materials with low RI, this study proposes the development of a refractometer based on a CYTOP optical fiber with LMR. To accomplish this objective, the work was divided into two parts: theoretical and experimental. In the theoretical part, simulations were conducted to determine the necessary thickness of the metallic oxide film to obtain the 1st- and 2nd-order LMRs. Furthermore, the simulations also provided insights into the sensitivity of each LMR. In the experimental part, the 1st- and 2nd-order LMRs were successfully generated by using D-shaped CYTOP fiber deposited with a thin film, based on the information obtained from the simulations. Subsequently, experimental tests were performed to evaluate the sensitivity of the refractometer both in the visible region (VIS) and in the NIR region. The material of the thin film used to obtain the LMR was SnO_2, given the high sensitivity and the stability it provides over time [20], [25].

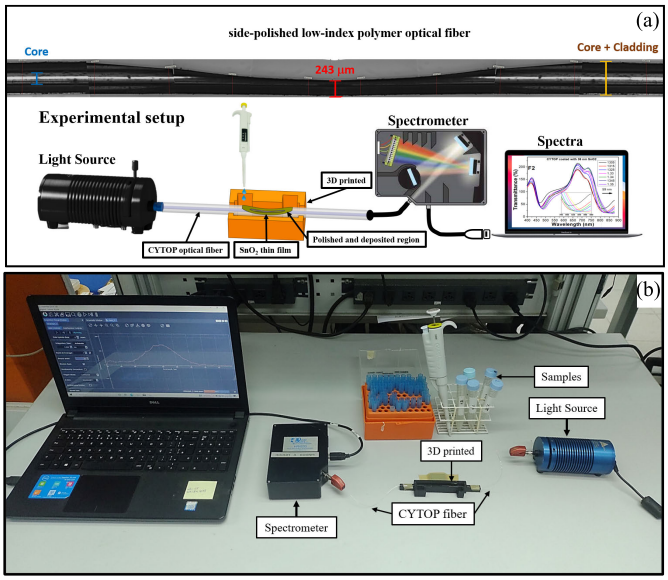

Fig. 1. (a) Illustrative drawing of the experimental setup used in this work to assess the sensor's performance, along with a micrograph (composite of various sections of the polished fiber) showing the CYTOP in its polished region. (b) Actual photograph of the experimental setup used to assess the performance of the sensor based on polished CYTOP fiber and SnO_2 thin film.

II. Materials and Methods

A. Materials

The refractometer presented in this study was constructed using a CYTOP optical fiber (GigaPOF120SR, Thorlabs), which underwent a polishing process and was subsequently coated with a thin film. The CYTOP fiber with a core and cladding of 120 and 490 μm, respectively, was side polishing until it reached a thickness of 243 μm (having the core exposed), as illustrated in Fig. 1(a).

The polishing process involved two types of sandpaper with grit sizes of 2000 and 5000 for the initial and intermediate polishing stages, respectively. Final polishing was completed using a 3-μm polishing film (Fiber Instrument Sales) to achieve a smoother surface finish. During polishing, the light loss in CYTOP was monitored to ensure repeatability in the process. In the initial stage, the light loss amounted to 10% (almost exposing the core), in the intermediate stage, the light loss was 50% (core exposed), and in the final stage, the focus was on reducing the roughness of the polished region.

To generate the LMR, an oxygen depleted black tin oxide target from Plasmaterials, referred to as SnO_{2-x}, was used. Nevertheless, for greater understanding, it is referenced in the work as SnO_2. The diameter of the target was 2 in and it was

placed inside a dc-sputtering machine. The CYTOP fiber was positioned 10 cm away from the target to mitigate the effects of plasma-induced heating. In the deposition process, the vacuum pressure was initially reduced to 5×10^{-3} mbar (without argon). Subsequently, a constant flow of argon was introduced into the chamber until the vacuum pressure reached 2×10^{-2} mbar. A current of 140 mA and a voltage of 220 V were used for starting deposition. The deposition process time varied based on the desired thickness of the SnO_2 film to obtain the 1st and 2nd LMR. These values were determined from the simulation results. Similar to the polishing process, the CTYOP spectrum was continuously monitored during the thin film deposition to ensure process repeatability.

To assess the performance of the LMRs, the experimental setup depicted in Fig. 1(b) was employed. In this configuration, a white light source (HL-2000, Ocean Insight) was connected to one end of the CYTOP fiber, while a spectrometer (HR4000, VIS region–Nirquest, NIR region) was connected to the other end. In addition, a 3-D-printed piece was employed to fix the fiber and leave the deposited region within the structure. The piece was designed with two cavities, allowing for the introduction and removal of the liquid used in the refractometer's characterization process. The experiments were conducted at room temperature (26 °C).

B. Simulation

A modified theoretical model based on SPR was utilized to simulate the LMRs in CYTOP fiber [26], [27]. In this adapted model, the ATR technique was employed using a Kretschmann configuration to obtain the transmitted optical power. This power is dependent on both the wavelength and the incident angle, denoted as $R\ (\theta,\ \lambda)$. One factor to consider in the simulation is the number of reflections $N(\theta)$, which depends on the film length, fiber core diameter, and angle of incidence.

Considering the aforementioned information, the transmitted power is calculated by solving the following equation:

$$T(\lambda) = \frac{\int_{\theta_c}^{90^\circ} p(\theta) R^{N(\theta)}(\theta, \lambda) d\theta}{\int_{\theta_c}^{90^\circ} p(\theta)} \tag{1}$$

where $R^{N(\theta)}(\theta, \lambda)$ denotes the reflected light, which comprises the combined reflection from both TE and TM mode polarizations, while θ_c stands for the critical angle [27].

The visualization of TE and TM polarization modes depends on several factors, including the RI of the SnO_2, the RI of the CYTOP fiber core, the RI of the SM, and the wavelength. The real part of the RI of SnO_2, ranging from 1.942 to 1.845 in the 400–1000-nm wavelength range, was determined using an ellipsometer (UVISEL 2, Horiba). The ellipsometer had a spectral range of 0.6–6.5 eV (190–2100 nm), an angle of incidence set at 70°, a 1-mm spot size, and utilized DeltaPsi2TM software (Horiba Scientific Thin Film Division) for data analysis. The ellipsometer also indicated a null imaginary part in the RI. However, as stated in a previous publication [28], the ellipsometer's angle of incidence was 70°. This choice was based on the pursuit of greater accuracy, as results tend to be more precise when the angle approaches the Brewster angle.

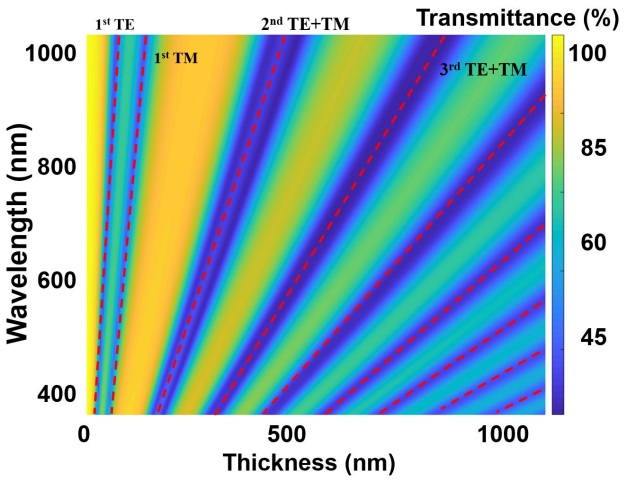

Fig. 2. Simulation results of a CTYOP fiber coated with SnO_2, with the thickness of the coating varying from 0 to 1100 nm. A video illustrating the changes in the optical spectrum as the deposition process takes place on the CYTOP can be seen in Visualization 1 in the Supplementary Material.

Moreover, this specific angle of incidence is recommended by the manufacturer (Horiba) for the material utilized in our experimental setup. Conversely, in the planar configuration, light is guided at a grazing incidence (90°) concerning the thin film, resulting in increased light scattering. Consequently, it is necessary to consider a higher imaginary part. For this purpose and considering that the imaginary part of the RI of the thin film is a parameter closely related to the LMR depth [17], [21], the simulated depth of the LMR was compared with the experimental depth for different values of the imaginary part. The value that best fits the experimental results was 0.03.

Similarly, Cao et al. [23] presented the dispersion curve of the CYTOP fiber RI in relation to the wavelength, and this information was incorporated into our simulation.

III. Results and Discussion

A. Simulation Results

To simulate LMRs in CYTOP fiber, the following data were used to obtain the results presented in Figs. 2 and 3: the RI of SnO_2 [28], the dispersion curve of the CYTOP RI fiber with respect to wavelength [23], and the RI dispersion data of water and glycerin [29], [30]. Fig. 2 illustrates the changes in the optical spectrum as the thickness of the simulated coating on the CYTOP fiber varies over time. In this simulation, an air medium was used as the surrounding RI, with a fiber core diameter of 100 μm. This value was used because the diameter of the CYTOP fiber is 120 μm and the fiber is side polished up to the center of the core approximately. Therefore, 100 μm is approximately an average value between these two extreme cases. It is important to note that in the simulation, if the core is either 90 or 100 μm, there will be no difference in sensitivity, but there would be variations in the full-width at half-maximum (FWHM) and the attenuation caused by the LMR. Since the simulation's primary goal is to determine sensitivity, we have opted for a polished core with a 100 μm diameter.

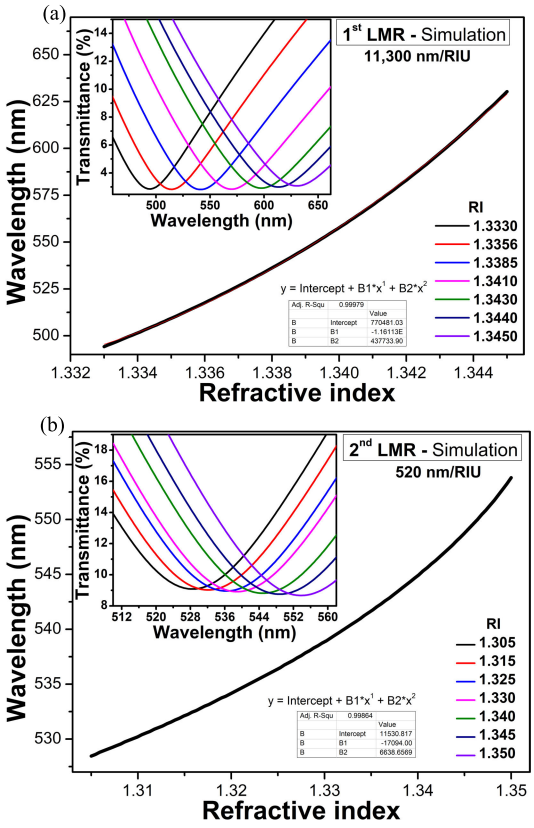

Fig. 3. Simulation results for the 1st and 2nd LMR. (a) Calculation of the sensitivity of the 1st LMR. (b) Calculation of the sensitivity of the 2nd LMR.

In addition, the thickness of the coating varied from 0 to 1100 nm and the results were analyzed within the wavelength range of 400–1000 nm, as depicted in Fig. 2. The color bar on the right of the figure represents the light intensity in percentage, with 100% indicating the maximum intensity.

The results indicate that the TE and TM components of the 1st LMR can be observed in the range from 400 to 1000 nm for small thickness values (the TE starts to be observed for 30 nm and the TM for 60 nm) and become visible between 400 and 800 nm. Furthermore, it was observed that the 1st LMR experiences a significant redshift with increasing thickness. In contrast, the 2nd LMR exhibits a slower redshift, which means less sensitivity but capability to monitor a parameter in a wider range as well as a more precise tuning of the LMR position. The 2nd LMR is visible in both the TE and TM components, nearly overlapping, at a thickness of 180 nm. Furthermore, Fig. 2 shows the presence of other LMR modes that are visible in the range from 400 to 1000 nm when the thickness exceeds 300 nm. These simulation results contrast with those reported in the literature, as the 2nd LMR appears in our simulations with a film deposition approximately six times larger than that required for the 1st LMR. This is in contrast to a multimode optical fiber of silica, where a little more than twice the deposition is needed to facilitate the transition from the 1st to the 2nd LMR [20].

In the simulation, the surrounding medium is initially considered as air (RI = 1.000), and once the required thickness of the thin film to achieve the first LMR is determined, the surrounding medium is then changed to 1.333, which corresponds to the RI of water. However, considering the anticipated high sensitivity of the sensor due to the low RI of the fiber core, it became necessary to reduce the thickness of the film. The results indicate that the spectrum of the 1st LMR emerges at approximately 500 nm when the thickness is 10 nm, as depicted in Fig. 3(a). To assess the sensitivity of the 1st LMR, the RI was varied from 1.3330 to 1.3450, and the corresponding results are presented in Fig. 3(a). Based on Fig. 3(a), it can be observed that the LMR sensitivity was 11 300 nm/RIU for RI values between 1.3330 and 1.3450.

To achieve the spectrum of the 2nd LMR close to the wavelength of 500 nm, a coating of 210 nm of SnO_2 was simulated. Given that the 2nd LMR tends to be less sensitive than the 1st LMR, a wider range of RIs was used to characterize it: 1.305–1.350. The simulation results are depicted in Fig. 3(b). As depicted in Fig. 3(b), the 2nd LMR exhibits a significantly smaller wavelength shift compared to the 1st LMR due to its lower sensitivity, which is up to 20 times lower. The sensitivity of the 2nd LMR was 514 nm/RIU within the RI range of 1.305–1.350.

B. Experimental Results

After the polishing process, the CYTOP fiber underwent characterization using a confocal microscope (Zeiss, LSM 900) to assess the depth of polishing and verify if a portion of the core extended beyond the cladding, as observed in Fig. 1(a). This analysis aimed to ensure the desired dimensions and geometry of the fiber were achieved. The polishing process was replicated on five CYTOP fibers to ensure the consistency and repeatability of the results. Experimental findings have indicated that a polishing level exceeding that illustrated in Fig. 1(a) results in excessive attenuation, preventing transmittance in the NIR range. Therefore, a suitable polishing process is achieved when the polished region has a diameter of 243 μm.

After the microscopic characterization, the CYTOP fiber was positioned on a 3-D-printed support [as shown in Fig. 1(b)] for testing with aqueous solutions of different RIs. For these tests, seven aqueous solutions were prepared by mixing double deionized water with sucrose at different percentages. The results of the characterization with aqueous solutions can be seen in Fig. 4. The results demonstrated that the polished CYTOP fiber exhibited a sensitivity exceeding 6600%/RIU within the range of 1.333–1.345, the highest attained with intensity-based sensors according to the review published by Urrutia et al. [1]. These findings suggest that the CYTOP fiber has the potential to be utilized as a sensor by leveraging changes in light power (light losses) as a detection mechanism. While the primary objective of this work is to study the LMR, evaluating the sensitivity of CYTOP (intensity-based) provides valuable insights that aid in standardizing the polishing process.

Table I presents the sensitivities of various POFs reported in the literature, which employ the light loss principle to measure the RI changes in aqueous media. The sensitivities of these POFs are compared with the polished CYTOP fiber, and the results demonstrate that CYTOP exhibits a sensitivity almost four times greater than the best one. Although the RI ranges

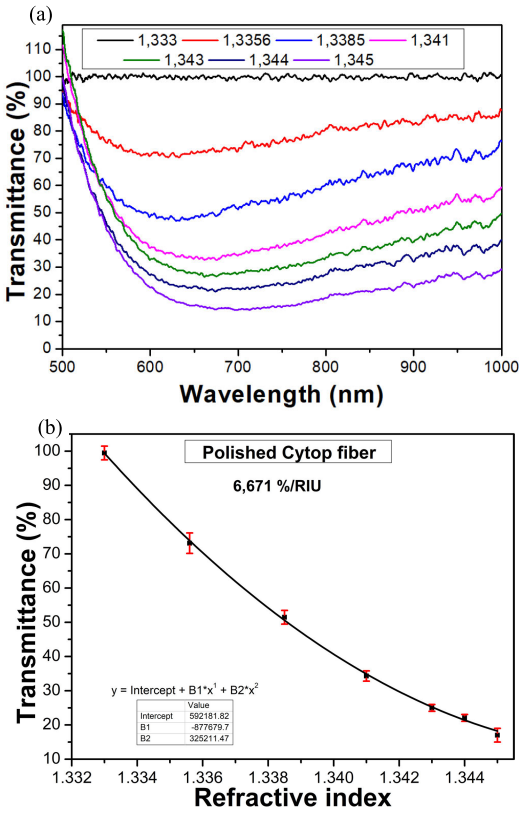

Fig. 4. (a) Transmittance spectrum obtained by immersing the polished CYTOP fiber in aqueous solutions with RI ranging from 1.333 to 1.345. (b) Calculation of CYTOP sensitivity was performed using the transmittance value at 700 nm.

TABLE I

SENSITIVITY OF THE POF REPORTED IN THE LITERATURE COMPARED WITH THE SENSITIVITY OF THE POLISHED CYTOP FIBER

Configuration	Sensitivity	Range	Ref.
Macrobending Tapered	937 %/RIU	1.333-1.410	[33]
Twisted Tapered	1,700 %/RIU	1.370-1.411	[34]
Side-Polished Macrobending	981 %/RIU	1.333-1.440	[35]
Double Side-Polished U-Shaped	1,541 %/RIU	1.333-1.390	[35]
FO2-shaped POF	904 %/RIU	1.333-1.381	[15]
Polished CYTOP fiber	6,671 %/RIU	1.333-1.345	This work

tested were different, it is important to mention that, for some biosensors, the ideal is that the highest sensitivity is achieved at an RI close to water (1.3330) because this way it is possible to detect analytes in low concentrations. A notable example is water contaminated with Escherichia coli or Salmonella [31], [32].

After polishing, the CYTOP was placed inside the dc-sputtering machine to perform SnO_2 coating on the polished region of the fiber. Before depositing the 1st- and 2nd-order LMR, one of the polished fibers was coated for 160 min to determine the deposition rate of SnO_2 and to establish a correlation between the deposition time and the previously simulated thickness (Fig. 2). Considering that a

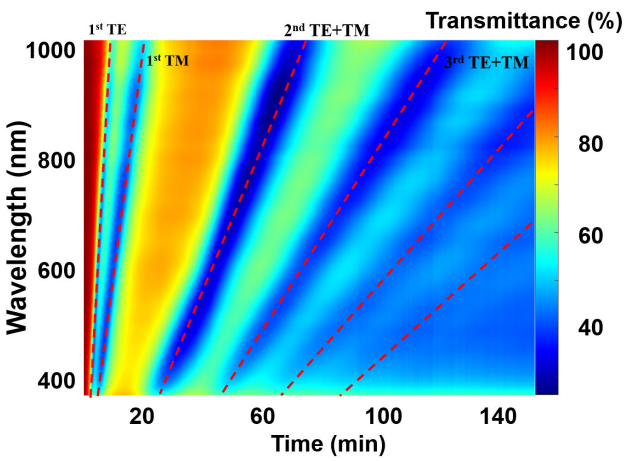

Fig. 5. Results of SnO_2 deposition onto polished CTYOP fiber using a dc-sputtering machine. The fiber was deposited continuously for 160 min to determine the times when the LMRs appeared.

thickness of 1100 nm was simulated for the same color map, the deposition rate is 6.875 nm/min.

As shown in Fig. 5, the emergence of the 1st LMR at both TE and TM was observed within 5 and 10 min, respectively. According to the estimated deposition rate, these values indicate 34.37 and 68.75 nm, values that agree well the 30 and 60 nm estimated with the simulations in Fig. 2. This indicates a good linearity in the deposition.

During the deposition process, the polished CYTOP fiber was monitored using a white light source [depicted in Fig. 1(b)] and the HR4000 spectrometer, enabling monitoring in the VIS region. Modifications were made to the dc-sputtering system to incorporate two optical fibers inside, facilitating communication between the light source and the spectrometer, which were located outside the sputtering chamber.

Based on the information extracted from Fig. 5, along with the simulation results shown in Fig. 2, it was determined that to achieve the 1st LMR in the VIS region in a solution with an RI of 1.333, the deposition time must be approximately 1.5 min. This corresponds to one-third of the time required to obtain the 1st LMR in air (RI = 1.000). Furthermore, by analyzing the results from Fig. 5, it was observed that the 2nd LMR in the VIS region appeared after 25 min. Its red shift occurred slowly, enabling more precise tuning. Additionally, due to its sensitivity to the RI being 20 times lower than that of the 1st LMR, it was determined that when transitioning from air to an aqueous solution, the LMR would experience a shift of 200 nm.

Fig. 6(a) displays the results obtained from the deposition and characterization of the 1st LMR in the VIS region. The 1st LMR was achieved by depositing a 10-nm SnO_2 film, corresponding to a deposition time of 1.5 min using the conditions described in the "Experimental Section." After depositing the 1st LMR, the fiber was positioned in the experimental setup depicted in Fig. 1(b) to characterize it with aqueous solutions, with the RI varying from 1.3330 to 1.3450.

The experimental results demonstrated that the CYTOP-fiber-based refractometer exhibited an exponential increase

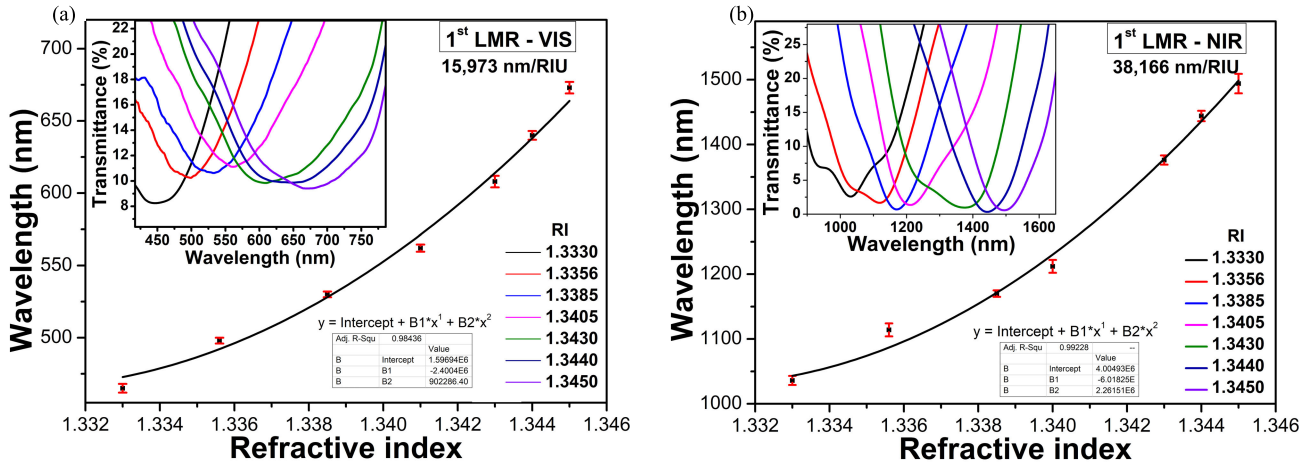

Fig. 6. Experimental results of characterization of sensors when submerged in liquids with RI from 1.3330 to 1.3450. (a) Characterization of the 1st LMR in the VIS region and (b) characterization of the 1st LMR in the NIR region.

in sensitivity, reaching high sensitivities exceeding 15 000 nm/RIU in the VIS region for RIs ranging from 1.3330 to 1.3450. Notably, in the range from 1.3405 to 1.3450, the sensitivity surpasses 26 000 RIU. This result aligns with the simulation findings, indicating that the proposed sensor exhibits high sensitivity even when tested in the VIS region. The difference between the experimental and theoretical sensitivities can be attributed to the information provided in the CYTOP datasheet from the manufacturer (Thorlabs). The datasheet specifies that the RI of the CYTOP can vary from 1.342 to 1.356, but no information is given on the specific values of RI at each wavelength. Therefore, in the simulation we used the model published in Cao et al. [23], which accounts for the dispersion but is less precise than extracting the values experimentally from the fiber itself. Consequently, due to the high sensitivity of the sensor, this has an impact on the agreement between the theoretical and experimental results. In any case, to the best of our knowledge, refractometers based on optical fibers in the VIS region typically demonstrate sensitivities up to 6000 nm/RIU.

To fine-tune the 1st LMR in the NIR region, the fiber was subjected to an additional 1-min deposition, resulting in a redshift that positions the LMR in a wavelength close to 1000 nm, as depicted in Fig. 6(b). The fiber was once again positioned in the experimental configuration depicted in Fig. 1(b) to characterize it with aqueous solutions. The results demonstrated that the refractometer exhibited a high sensitivity, surpassing 38 000 nm/RIU within the RI range of 1.3330–1.3450. Additionally, it achieved a sensitivity exceeding 57 000 nm/RIU for RIs greater than 1.340.

Table II shows a comparison of the sensitivities of sensors reported in the literature with the sensor proposed in this study. The results indicate that the sensor proposed in this work ranks as one of the most sensitive sensors among optical fiber-based refractometers in a range close to water (RI = 1.333), being four times more sensitive than the LMR-based refractometer with fiber optics. In comparison to the CYTOP fiber coated with a gold film (utilizing SPR), the proposed refractometer demonstrated a sensitivity that exceeded it by a factor of 2.4 [23]. Furthermore, according to the review on optical fiber refractometers by Urrutia et al. [1], the sensitivity attained is the highest in the water region (only a few sensors operating in the silica RI region, typically more sensitive, exceed the 57 000 nm/RIU sensitivity obtained here). It is important to mention that the achieved record falls within the RI range of phosphate-buffered saline (PBS, RI = 1.34). PBS is commonly used as a matrix in bioassays, as many biological analytes are diluted in it. Moreover, its maximum sensitivity can also be leveraged for detecting contaminants in water, given that the RI of water is 1.33. In other words, in a biosensor application, the proposed sensor based on CYTOP and LMR would operate in the region of maximum sensitivity.

In order to perform a complete characterization, a thicker film of SnO_2 was deposited on the polished CYTOP fiber to obtain the 2nd LMR. The film thickness was 206 nm (30-min deposition) to tune the 2nd LMR at 560 nm in water (this value agrees well with the 210 nm of the simulation shown in Fig. 3). Once the 2nd LMR was deposited, the fiber was again placed in the 3-D piece illustrated in Fig. 1(b) for characterization with aqueous solutions.

Fig. 7 illustrates the results obtained from testing the 2nd LMR at different wavelengths. For this purpose, the sensor was progressively deposited to finely tune the LMR to the desired wavelength. Table III shows the sensitivity results related to the spectral position of the LMR. Based on the results, it is observed that the sensitivity of the LMR increases proportionally with the wavelength position of the LMR, which is consistent with the findings reported in [17]. The sensitivities achieved, exceeding 3000 nm/RIU for the 2nd LMR within the RI range of 1.3330–1.3405 [see Fig. 7(d)] and 5083 nm/RIU for RIs greater than 1.3400, set a new record for fiber optic-based refractometers utilizing the 2nd LMR.

In addition, a notable similarity was observed in the calculated sensitivities after comparing the experimental results [Fig. 7(a)] with the simulation results [Fig. 2(b)]. The simulation indicated a sensitivity of 520 nm/RIU in the VIS region, while the experiments demonstrated a sensitivity of 467 nm/RIU within the same range of RIs.

TABLE II
COMPARISON BETWEEN VARIOUS LMR-BASED (OR SPR-BASED) SENSORS

Sensor	Coating	Range of RI	Spectral region	Sensitivity	Ref.
200 µm – MM	ITO	1.332–1.436	NIR	3,125 nm/RIU	[36]
200 µm – MM	In_2O_3	1.33–1.37	NIR	4,926 nm/RIU	[37]
SM-MM-SM	AZO	1.365-1.400	NIR	1,214 nm/RIU	[38]
200 µm – MM	CuO	1.333-1.407	NIR	7,234 nm/RIU	[39]
200 µm – MM	GO-PEI	1.33-1.42	NIR	12,460 nm/RIU	[18]
D-shaped SM	IGZO	1.39-1.42	NIR	12,929 nm/RIU	[40]
200 µm – MM	SnO_2	1.33-1.41	NIR	5,390 nm/RIU	[20]
D-shaped SM	TiO_2	1.333-1.398	NIR	4,122 nm/RIU	[19]
CYTOP – SPR	Au	1.335	NIR	22,779 nm/RIU	[23]
MZ – SPR	Au	1.335-1.385	VIS	1,947 nm/RIU	[16]
PFA planar waveguide	ITO	1.3318-1.3347	NIR	41,034 nm/RIU	[25]
Polished CYTOP fiber	SnO_2	1.3405-1,3450	VIS	26,311 nm/RIU	This work
		1.3405-1.3450	NIR	57,200 nm/RIU	
		1.3330-1.3450	VIS	15,973 nm/RIU	
		1.3330-1.3450	NIR	38,166 nm/RIU	

MM: multimode fiber; SM: single-mode fiber; NMF: nano-modified fiber optic; MZ: Mach–Zehnder interference;

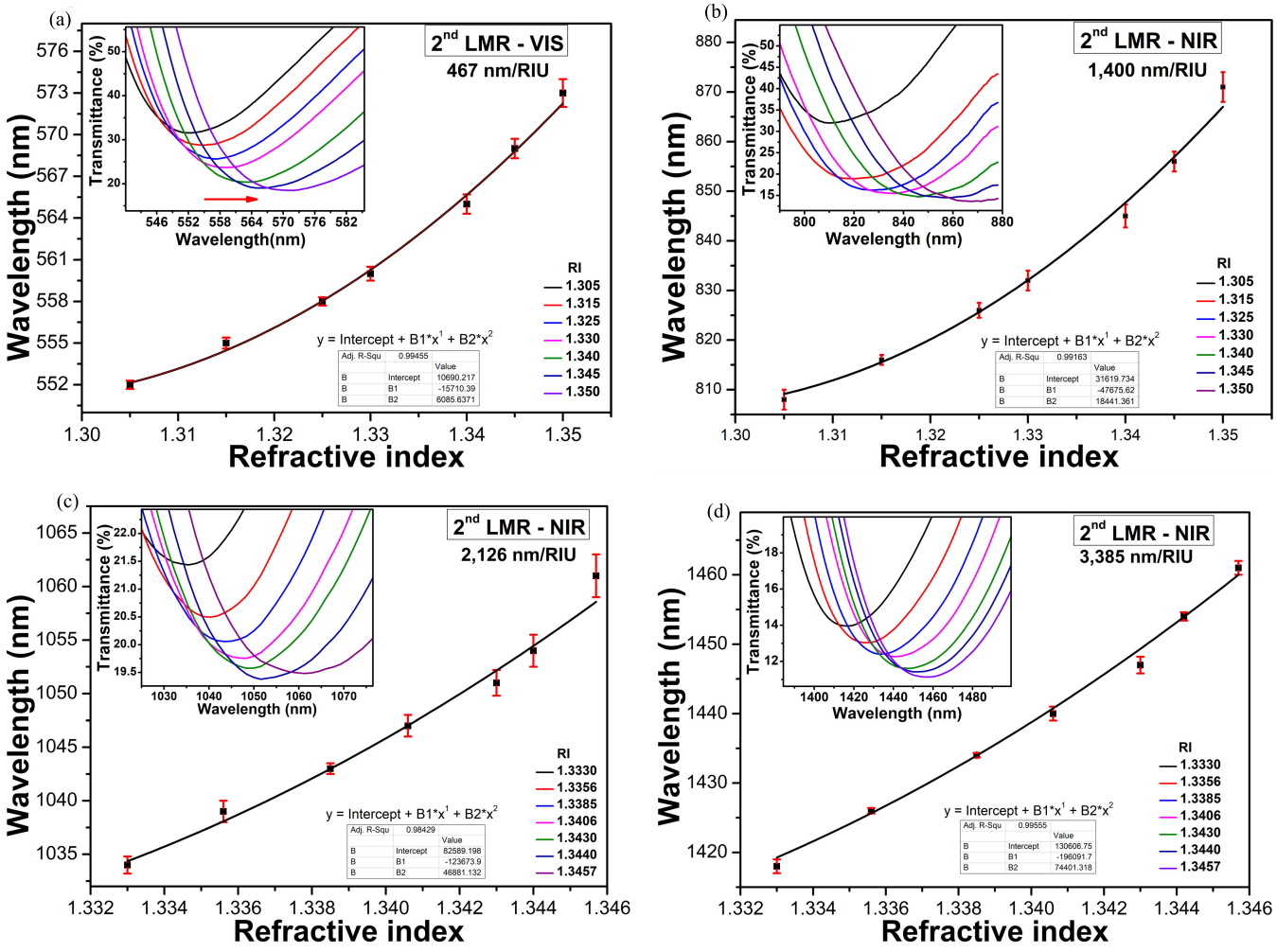

Fig. 7. Experimental results of the sensitivity of the 2nd LMR analyzed at the following wavelengths (a) 550, (b) 805, (c) 1030, and (d) 1415 nm.

The sensor proposed in this work has great potential in the area of biosensors because its high sensitivity is tuned to the RI region where the PBS commonly, used as a matrix in bioassays, is located, or in the domain of detection of contaminants in water (the water RI is 1.33). Additionally, it offers a cost-effective production process with good repeatability. Another thing to highlight is that the polished CYTOP has an easier polishing process when compared with the traditional D-polished single-mode fiber. However, one of the limitations of CYTOP fiber is its applicability in domains, where the surrounding medium RI is higher than the RI of CYTOP, such as the oil industry. This is due to the fact that oil typically has

TABLE III
SENSITIVITY VARIATION BASED ON THE SPECTRAL POSITION OF THE 2ND LMR WAVELENGTH

Wavelength (nm)	Sensitivity (nm/RIU)
540	467
808	1,400
1034	2,126
1212	2,900
1417	3,385

an RI greater than 1.44, which exceeds the RI of CYTOP, making its use unfeasible.

IV. CONCLUSION

This work presented a refractometer based on a side-polished low-index polymer optical fiber (the polymer used was CYTOP), both with and without a coating. The refractometer without SnO_2 coating had a high sensitivity of more than 6600%/RIU, positioning it as the most sensitive intensity-based RI sensor in the literature. Likewise, the refractometer based on 1st and 2nd LMR (the nanocoating was SnO_2) had a high sensitivity of more than 57 000 nm/RIU and more than 5000 nm/RIU, for the 1st and 2nd LMR, respectively. The remarkable sensitivity achieved with LMRs in this study highlights their potential as an alternative to SPRs in applications that require low detection limits, particularly biosensors. Moreover, the progressive increase of the sensitivity as a function of the wavelength position of the same LMR in the VIS and NIR spectral region, easily attained by controlling the nanocoating thickness, demonstrated the capability to tune the performance of this structure in a broad spectrum, something that is not possible with SPR-based sensors. In addition, the proposed sensor presents a viable substitute for LMR sensors based on D-shaped fiber. This research was supported by both simulation and experimental results, which exhibited strong correlation and yielded similar outcomes, and suggests that CYTOP fibers could be used in applications, where very low limit of detection is required, such as biosensors and chemical sensors.

CREDIT AUTHORSHIP CONTRIBUTION STATEMENT

Juan David Lopez: Conceptualization, methodology, investigation, simulation, formal analysis, and writing-original draft. Ignacio R. Matias: Project administration, supervision, funding acquisition, investigation, methodology, writing-review and editing, and visualization. Regina Célia da Silva Allil: Funding acquisition and visualization. Marcelo Martins Werneck: Supervision, funding acquisition, visualization, and review. Ignacio Del Villar: Project administration, supervision, funding acquisition, investigation, methodology, simulation, writing-review and editing, and visualization. All authors have read and agreed to the published version of the manuscript.

DECLARATION OF COMPETING INTEREST

The authors declare no competing financial interest.

REFERENCES

[1] A. Urrutia, I. Del Villar, P. Zubiate, and C. R. Zamarreño, "A comprehensive review of optical fiber refractometers: Toward a standard comparative criterion," *Laser Photon. Rev.*, vol. 13, no. 11, Nov. 2019, Art. no. 1900094, doi: 10.1002/lpor.201900094.

[2] A. Ozcariz, C. Ruiz-Zamarreño, and F. J. Arregui, "A comprehensive review: Materials for the fabrication of optical fiber refractometers based on lossy mode resonance," *Sensors*, vol. 20, no. 7, p. 1972, Apr. 2020, doi: 10.3390/s20071972.

[3] C. Leitão et al., "Cost-effective fiber optic solutions for biosensing," *Biosensors*, vol. 12, no. 8, p. 575, Jul. 2022, doi: 10.3390/bios12080575.

[4] M. Li, R. Singh, Y. Wang, C. Marques, B. Zhang, and S. Kumar, "Advances in novel nanomaterial-based optical fiber biosensors—A review," *Biosensors*, vol. 12, no. 10, p. 843, Oct. 2022, doi: 10.3390/bios12100843.

[5] A. Kumar Shakya and S. Singh, "State of the art in fiber optics sensors for heavy metals detection," *Opt. Laser Technol.*, vol. 153, Sep. 2022, Art. no. 108246, doi: 10.1016/j.optlastec.2022.108246.

[6] Z. Heidarnia, R. Parvizi, H. Khoshsima, and H. Heidari, "Distinct absorption transducing features of silica supported MoO_3/PANI hybrid coated optical fiber towards malathion monitoring in food samples," *Sens. Actuators B, Chem.*, vol. 371, Nov. 2022, Art. no. 132501, doi: 10.1016/j.snb.2022.132501.

[7] Z. Ran et al., "Fiber-optic microstructure sensors: A review," *Photonic Sensors*, vol. 11, no. 2, pp. 227–261, Jun. 2021, doi: 10.1007/s13320-021-0632-7.

[8] H. Liang, J. Wang, L. Zhang, J. Liu, and S. Wang, "Review of optical fiber sensors for temperature, salinity, and pressure sensing and measurement in seawater," *Sensors*, vol. 22, no. 14, p. 5363, Jul. 2022, doi: 10.3390/s22145363.

[9] L. Rodriguez-Saona, D. P. Aykas, K. R. Borba, and A. Urtubia, "Miniaturization of optical sensors and their potential for high-throughput screening of foods," *Current Opinion Food Sci.*, vol. 31, pp. 136–150, Feb. 2020, doi: 10.1016/j.cofs.2020.04.008.

[10] F. Chiavaioli et al., "Ultrahigh sensitive detection of tau protein as Alzheimer's biomarker via microfluidics and nanofunctionalized optical fiber sensors," *Adv. Photon. Res.*, vol. 3, no. 11, Nov. 2022, Art. no. 2200044, doi: 10.1002/adpr.202200044.

[11] X. Zhang et al., "Side-polished SMS based RI sensor employing macrobending perfluorinated POF," *Opto-Electron. Adv.*, vol. 4, no. 10, 2021, Art. no. 200041, doi: 10.29026/oea.2021.200041.

[12] Y. Singh, M. T. I. Ansari, and S. K. Raghuwanshi, "Design and development of titanium dioxide (TiO_2)-coated eFBG sensor for the detection of petrochemicals adulteration," *IEEE Trans. Instrum. Meas.*, vol. 70, pp. 1–8, 2021, doi: 10.1109/TIM.2021.3053985.

[13] S.-I. Takeda, M. Sato, and T. Ogasawara, "Simultaneous measurement of strain and temperature using a tilted fiber Bragg grating," *Sens. Actuators A, Phys.*, vol. 335, Mar. 2022, Art. no. 113346, doi: 10.1016/j.sna.2021.113346.

[14] C. Teng et al., "Intensity-modulated polymer optical fiber-based refractive index sensor: A review," *Sensors*, vol. 22, no. 1, p. 81, Dec. 2021, doi: 10.3390/s22010081.

[15] J. D. Lopez, A. Dante, R. C. da Silva Allil, and M. M. Werneck, "The influence of geometric shape on the performance of refractive index sensors based on plastic optical fibers: Simulations and experimental assessment," *IEEE Sensors J.*, vol. 23, no. 6, pp. 5803–5809, Mar. 2023, doi: 10.1109/JSEN.2023.3240292.

[16] R.-J. Tong, Y. Wang, K.-J. Zhao, and Y. Zhao, "Surface plasmon resonance optical fiber sensor for refractive index detection without temperature crosstalk," *IEEE Trans. Instrum. Meas.*, vol. 71, pp. 1–6, 2022, doi: 10.1109/TIM.2022.3157392.

[17] W.-M. Zhao and Q. Wang, "Analytical solutions to fundamental questions for lossy mode resonance," *Laser Photon. Rev.*, vol. 17, no. 1, 2022, Art. no. 2200554, doi: 10.1002/lpor.202200554.

[18] M. Hernaez, A. G. Mayes, and S. Melendi-Espina, "Lossy mode resonance generation by graphene oxide coatings onto cladding-removed multimode optical fiber," *IEEE Sensors J.*, vol. 19, no. 15, pp. 6187–6192, Aug. 2019, doi: 10.1109/JSEN.2019.2906010.

[19] Vikas, S. Mishra, A. Mishra, P. Saccomandi, and R. Verma, "Recent advances in lossy mode resonance-based fiber optic sensors: A review," *Micromachines*, vol. 13, no. 11, p. 1921, Nov. 2022, doi: 10.3390/mi13111921.

[20] P. Sanchez, C. R. Zamarreño, M. Hernaez, I. R. Matias, and F. J. Arregui, "Optical fiber refractometers based on lossy mode resonances by means of SnO_2 sputtered coatings," *Sens. Actuators B, Chem.*, vol. 202, pp. 154–159, Oct. 2014, doi: 10.1016/j.snb.2014.05.065.

[21] I. Del Villar et al., "Optical sensors based on lossy-mode resonances," *Sens. Actuators B, Chem.*, vol. 240, pp. 174–185, Mar. 2017, doi: 10.1016/j.snb.2016.08.126.

[22] V. F. Cardoso, D. M. Correia, C. Ribeiro, M. M. Fernandes, and S. Lanceros-Méndez, "Fluorinated polymers as smart materials for advanced biomedical applications," *Polymers*, vol. 10, no. 2, p. 161, 2018, doi: 10.3390/polym10020161.

[23] S. Cao et al., "Highly sensitive surface plasmon resonance biosensor based on a low-index polymer optical fiber," *Opt. Exp.*, vol. 26, no. 4, pp. 3988–3994, 2018, doi: 10.1364/oe.26.003988.

[24] I. Dominguez, J. Corres, I. R. Matias, J. Ascorbe, and I. del Villar, "High sensitivity lossy-mode resonance refractometer using low refractive index PFA planar waveguide," *Opt. Laser Technol.*, vol. 162, Jul. 2023, Art. no. 109235, doi: 10.1016/j.optlastec.2023.109235.

[25] I. R. Matias, I. D. Villar, and J. M. Corres, "Lossy mode resonance-based sensors in planar configuration: A review," *IEEE Sensors J.*, vol. 23, no. 7, pp. 6397–6405, Apr. 2023, doi: 10.1109/JSEN.2023.3243937.

[26] A. K. Sharma and B. D. Gupta, "On the sensitivity and signal to noise ratio of a step-index fiber optic surface plasmon resonance sensor with bimetallic layers," *Opt. Commun.*, vol. 245, nos. 1–6, pp. 159–169, Jan. 2005, doi: 10.1016/j.optcom.2004.10.013.

[27] I. Del Villar et al., "Generation of lossy mode resonances by deposition of high-refractive-index coatings on uncladded multimode optical fibers," *J. Opt.*, vol. 12, no. 9, 2010, Art. no. 095503, doi: 10.1088/2040.8978/12/9/095503.

[28] E. Gonzalez-Valencia, I. D. Villar, and P. Torres, "Novel bloch wave excitation platform based on few-layer photonic crystal deposited on D-shaped optical fiber," *Sci. Rep.*, vol. 11, no. 1, May 2021, Art. no. 11266, doi: 10.1038/s41598-021-90504-z.

[29] J. Rheims, J. Köser, and T. Wriedt, "Refractive-index measurements in the near-IR using an abbe refractometer," *Meas. Sci. Technol.*, vol. 8, no. 6, pp. 601–605, Jun. 1997, doi: 10.1088/0957-0233/8/6/003.

[30] M. Daimon and A. Masumura, "Measurement of the refractive index of distilled water from the near-infrared region to the ultraviolet region," *Appl. Opt.*, vol. 46, no. 18, pp. 3811–3820, 2007, doi: 10.1364/ao.46.003811.

[31] A. B. Pebdeni, A. Roshani, E. Mirsadoughi, S. Behzadifar, and M. Hosseini, "Recent advances in optical biosensors for specific detection of *E. coli* bacteria in food and water," *Food Control*, vol. 135, May 2022, Art. no. 108822, doi: 10.1016/j.foodcont.2022.108822.

[32] M. Angelopoulou, K. Tzialla, A. Voulgari, M. Dikeoulia, I. Raptis, and S. E. Kakabakos, "Rapid detection of Salmonella typhimurium in drinking water by a white light reflectance spectroscopy immunosensor," *Sensors*, vol. 21, p. 2683, 2021, doi: 10.3390/s21082683.

[33] C. Teng, N. Jing, F. Yu, and J. Zheng, "Investigation of a macrobending tapered plastic optical fiber for refractive index sensing," *IEEE Sensors J.*, vol. 16, no. 20, pp. 7521–7525, Oct. 2016, doi: 10.1109/JSEN.2016.2601380.

[34] Teng et al., "Refractive index sensor based on twisted tapered plastic optical fibers," *Photonics*, vol. 6, no. 2, p. 40, Apr. 2019, doi: 10.3390/photonics6020040.

[35] N. Jing, J. Zhou, K. Li, Z. Wang, J. Zheng, and P. Xue, "Refractive index sensing based on a side-polished macrobend plastic optical fiber combining surface plasmon resonance and macrobending loss," *IEEE Sensors J.*, vol. 19, no. 14, pp. 5665–5669, Jul. 2019, doi: 10.1109/JSEN.2019.2908418.

[36] C. R. Zamarreno, M. Hernaez, I. Del Villar, I. R. Matias, and F. J. Arregui, "ITO coated optical fiber refractometers based on resonances in the infrared region," *IEEE Sensors J.*, vol. 10, no. 2, pp. 365–366, Feb. 2010, doi: 10.1109/JSEN.2009.2034628.

[37] C. R. Zamarreno et al., "Sensing properties of indium oxide coated optical fiber devices based on lossy mode resonances," *IEEE Sensors J.*, vol. 12, no. 1, pp. 151–155, Jan. 2012, doi: 10.1109/JSEN.2011.2142181.

[38] P. Prieto-Cortés, R. I. Álvarez-Tamayo, M. García-Méndez, and M. Durán-Sánchez, "Lossy mode resonance generation on sputtered aluminum-doped zinc oxide thin films deposited on multimode optical fiber structures for sensing applications in the 1.55 μm wavelength range," *Sensors*, vol. 19, no. 19, p. 4189, Sep. 2019, doi: 10.3390/s19194189.

[39] A. Ozcariz, I. Martinez, C. R. Zamarreño, and F. J. Arregui, "Development of copper oxide thin film for lossy mode resonance-based optical fiber sensor," *Proceedings*, vol. 2, no. 13, p. 893, 2018, doi: 10.3390/proceedings2130893.

[40] A. Ozcariz, M. Dominik, M. Smietana, C. R. Zamarreño, I. Del Villar, and F. J. Arregui, "Lossy mode resonance optical sensors based on indium-gallium-zinc oxide thin film," *Sens. Actuators A, Phys.*, vol. 290, pp. 20–27, May 2019, doi: 10.1016/j.sna.2019.03.010.

Juan David Lopez was born in Alcala Valle, Colombia. He received the Diploma degree in physical engineering from the Universidad Tecnologica de Pereira, Pereira, Colombia, in 2017, and the M.Sc. degree in nanotechnology engineering from the Federal University of Rio de Janeiro, Rio de Janeiro, Brazil, in 2020, where he is currently pursuing the Ph.D. degree in nanotechnology engineering.

He is a Researcher with the Photonics and Instrumentation Laboratory, Federal University of Rio de Janeiro (UFRJ), Rio de Janeiro, Brazil. His research interests include fiber optic sensors and nanomaterials.

Ignacio R. Matias (Fellow, IEEE) received the M.S. degree in electrical and electronic engineering and the Ph.D. degree in optical fiber sensors from the Polytechnic University of Madrid (UPM), Madrid, Spain, in 1992 and 1996, respectively.

He became a Lecturer with the Public University of Navarre, Pamplona, Spain, in 1996, where he is currently a Permanent Professor. He has coauthored more than 200 journals and 250 conference papers related to optical fiber sensors and passive optical devices and systems.

Marcelo Martins Werneck was born in Petrópolis, State of Rio de Janeiro, Brazil. He received the degree in electronic engineering from the Pontifícia Universidade Católica do Rio de Janeiro, Rio de Janeiro, (PUC-RJ), Brazil, in 1975, the M.Sc. degree in biomedical engineering from the Biomedical Engineering Program, Federal University of Rio de Janeiro (UFRJ), Rio de Janeiro, in 1977, and the Ph.D. degree in biomedical engineering from the University of Sussex, Brighton, U.K., in 1985.

He is currently a Lecturer and a Researcher with UFRJ and the Coordinator of the Photonics and Instrumentation Laboratory, Electrical Engineering Program, UFRJ. His research interests include nanosensors, fiber optic sensors, transducers, and instrumentation.

Regina Célia da Silva Allil was born in Rio de Janeiro, Brazil. She received the B.Sc. degree in electronic engineering from Faculdade Nuno Lisboa, Rio de Janeiro, in 1988, the M.Sc. degree from the Biomedical Engineering Program, Federal University of Rio de Janeiro (UFRJ), Rio de Janeiro, in 2004, and the D.Sc. degree from the Electronic Engineering Program, Instrumentation and Photonics Laboratory, UFRJ, in 2010.

She is a Researcher with the Brazilian Army Technological Center (CTEx), Rio de Janeiro, and the Instrumentation and Photonics Laboratory, UFRJ. Her research interests include fiber optics sensors, optoelectronic instrumentation, and biosensors.

Ignacio Del Villar received the M.S. degree in electrical and electronic engineering and the Ph.D. degree in optical fiber sensors from the Public University of Navarre (UPNA), Pamplona, Spain, in 2002 and 2006, respectively.

He has been an Associate Professor with UPNA, since 2021. His research interests include optical fiber sensors and the effect of nanostructured coatings deposited on waveguides, where he has coauthored more than 200 chapter books, journals, and conference papers.

Dr. Villar was an Associate Editor of the *Optics and Laser Technology* journal from 2012 to 2022. He has been an Associate Editor of *Sensors* journal since 2017.